

Supplementary material

In the supplementary material, we mainly present a few additional simulation results to complement what was presented in the paper. We showed simulations in the main text for the monostable switch model: here we present a selection of simulation results for the bistable switch case. Then we present a couple of additional simulations referred to in the text.

The tumour cell density distribution for the case of intrinsic drug resistances in the ODE (Fig.S1) and PDE (Fig.S2) model setting are shown below, followed by heterogeneous distribution of drug resistances (Fig.S3) as well as combined drug resistance mechanisms (both intrinsic and induced) in PDE setting (Fig.S4), under step signal. Overall, the simulation results display similar trends of tumour cell density distribution even though a qualitatively different intracellular apoptotic models was used. Similar conclusions hold good here too, and this complements what was discussed in the text. It indicates how many aspects of the interplay between the drug, the resistance mechanisms considered, and the responses, are not dependent on the details of the apoptosis model employed.

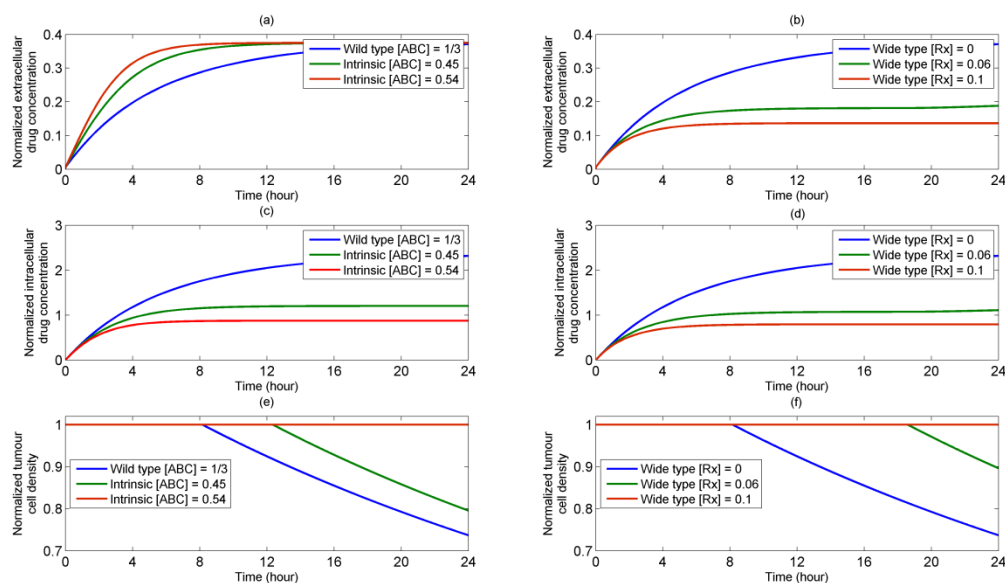


Fig.S1 Effect of intrinsic ABC transporter drug resistance (left column) and intrinsic internal detoxifying drug resistance (right column) on temporal profiles of (a) and (b) extracellular drug concentration, (c) and (d) intracellular drug concentration, and (e) and (f) tumour cell density under step infusion of drug intensity $S = 1.5$ (in dimensionless terms: see text for details) in the ODE-based model formulation.

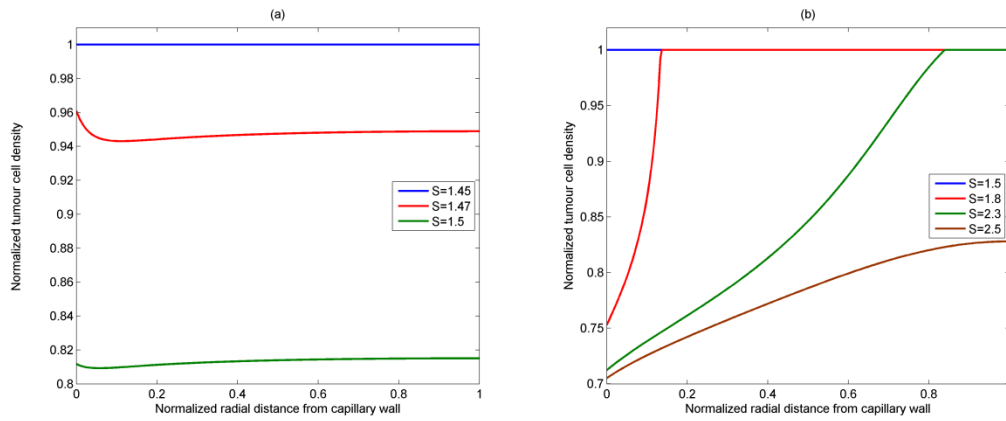


Fig.S2 Spatial profiles of tumour cell density at 24h under step infusion for varying signal intensity, (a) intrinsic ABC transporter drug resistance, (b) intrinsic internal resistance. The default concentrations of intrinsic ABC transporter and internal resistant proteins are set 0.45 and 0.1 respectively

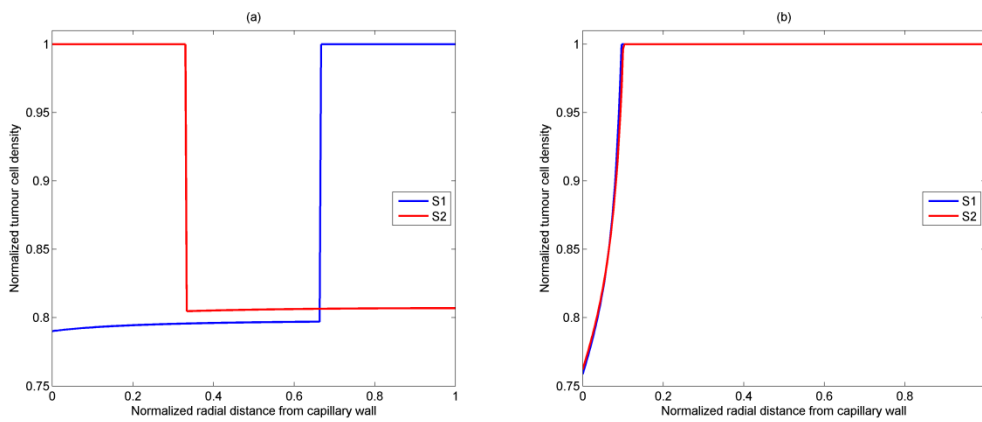


Fig.S3 Spatial profiles of tumour cell density at 24h for (a) heterogeneous distributions of intrinsic ABC transporter resistance under step infusion with signal intensity $S=1.8$ (b) heterogeneous distributions of intrinsic internal resistance under step infusion with $S=1.8$.

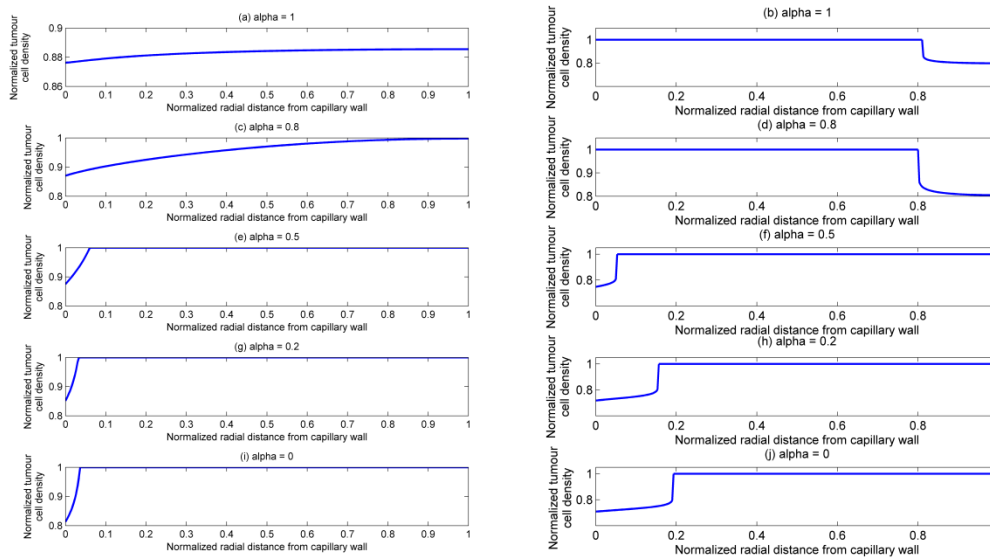


Fig.S4 Spatial profiles of tumour cell density at 24h, left column: combination of intrinsic ABC transporter and internal resistance under step infusion with signal intensity $S=1.6$; right column: combination of drug-induced ABC transporter and internal resistance under step infusion with signal intensity $S=2.2$.

Combined resistance mechanisms: response to pulse stimulation.

We have considered the response of a combination of resistance mechanisms to persistent infusion. For completeness here we show some simulations for the case of a pulse stimulus. It is shown in Fig.S5 below that (1) tissue response can be analyzed and predicted over a range that is largely determined by the dominant type of intrinsic drug resistance (for the case of combination of intrinsic resistances) and (2) in the case of combined induced resistances, a heterogeneous distribution of tumour cell density results in the internal induced mechanism being generally more dominating.

Varying intrinsic resistance:

We have discussed the effects of varying intrinsic resistance and indicated that a consistent picture emerges when one examines the effect of variation of stimulus for fixed resistance, and the effect of resistance for fixed stimulus. An example of the latter is shown in Fig. S6, where the effects of the intrinsic internal detoxifying mechanism is varied, keeping the stimulus fixed. The response of the tissue in general changes, but with a trend which can be predicted and is consistent with the variation of stimulus keeping resistance fixed.

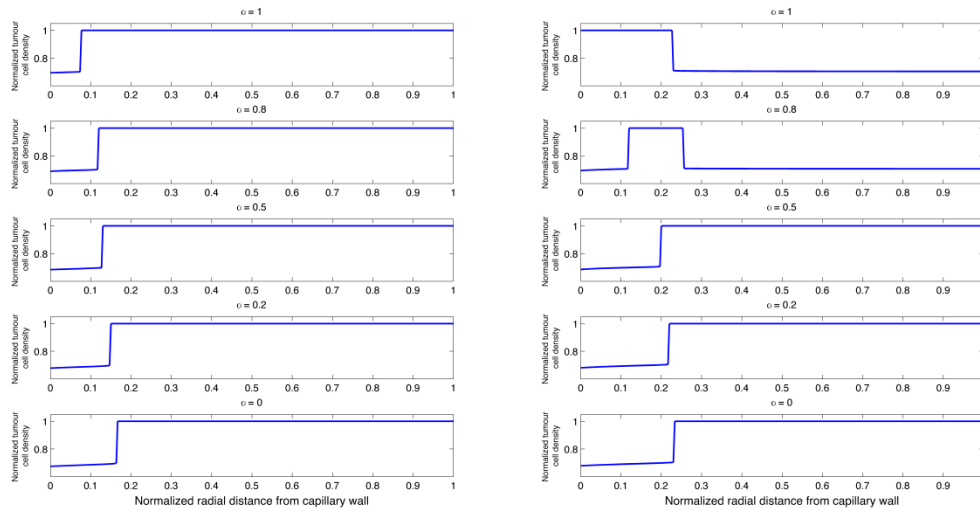


Fig.S5 Spatial profiles of tumour cell density at 24h, left column: combination of intrinsic ABC transporter and internal resistance under pulse injection (monostable switch case, considered in the text) with signal intensity $S=2.5$, $T=4h$; right column: combination of drug-induced ABC transporter and internal feedback resistance under pulse injection $S=2$, $T=5h$.

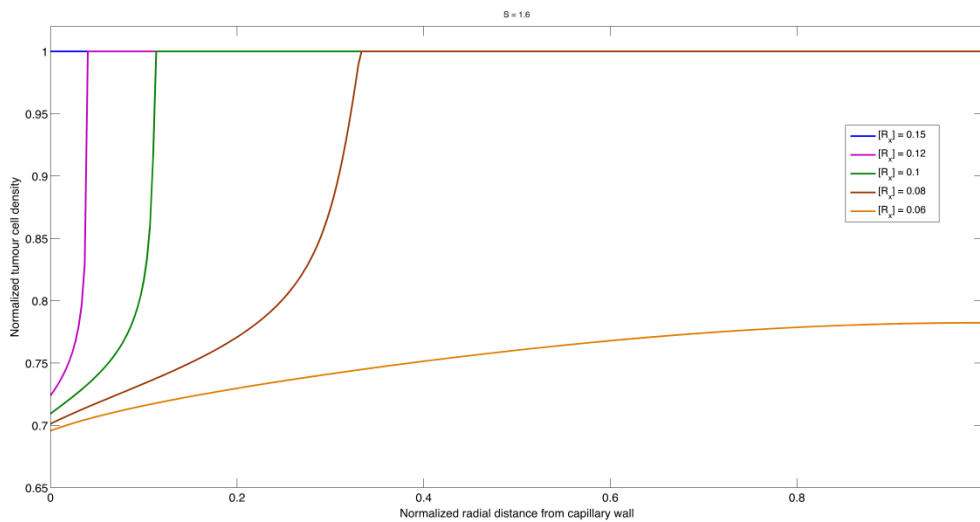


Fig.S6 Spatial profiles of tumour cell density at 24h under same conditions as Fig. 3(b), except that the internal detoxifying resistance parameter is varied for a fixed signal strength. A completely consistent pattern emerges from examining the effects of varying resistance (for fixed stimulus) and from varying stimulus (for fixed resistance strength). The value for this parameter of 0.1 corresponds to the baseline used in the text.

